Root Locus-Based Magnetic Levitation System Stabilization: An Undergraduate Control System Design Approach

[1]Katende, J.; [2]Awelewa, A.A.; [3]Samuel, I.A.; and [4]Iyiola, S.O.

[1]College of Technology, Botswana International University of Science & Technology, Gaborone, Botswana.
[2,3,4]Department of Electrical and Information Engineering, College of Science & Technology, Covenant University, Ota, Ogun State, Nigeria

Abstract

The subject of control system design has evolved considerably over the years. Although several design techniques and strategies have been adopted to realize control systems that meet a predetermined set of performance criteria, the fundamental problem remains that of developing controllers to adjust the performance characteristics of a dynamic system in order to obtain a desired output behavior. The dynamic behavior of a magnetic levitation system (MLS) of a ferromagnetic ball is compensated in this paper. Consolidating the exposure of undergraduate students to the rudiments of control system design, the paper employs the classical root locus technique to stabilize the system. A combination of analytical and software-based methods is used to design proportional-derivative and phase-lead compensators based on the linearized model of the system. Complete details of the design approach, from modeling and analysis of the plant to computing the values of the controller parameters, are shown. MATLAB scripts for plotting root loci and simulating the system are provided.

***Key words**: compensators, magnetic levitation system, MATLAB® scripts, modeling, root-locus method, system stability*

1. Introduction

The magnetic levitation system has attracted a great deal of attention both in the industry and academia. In the industry, significant applications, such as passenger train levitation, magnetic bearing, metal sheet levitation, protection of sensitive machinery, etc., have been recorded, while in the academia, authors of books on control systems theory (Franklin et al., 1998; Nise, 2007) have used similar versions of the system to educate undergraduate students on the subject of control systems, with laboratories having prototypes and experimental models of the system handy for instructional purposes (Naumivic and Veselic, 2008; Green et al., 1995). The magnetic levitation system of a ferromagnetic ball has a complex nonlinear dynamic equation, and its characteristic response inherently unstable (Feedback Instrument, 2012). Successful efforts have been made to design nonlinear controllers (Al-Muthairi and Zribi, 2004) just as well as linear controllers (Naumivic and Veselic, 2008; Green et al., 1995; Feedback Instrument, 2012) to stabilize the system. This latter type, which is further considered in this paper, is based on the linearized version of the system operating in a small range around an operating point. The aim of the paper is to shed more light on the use of a classical technique in stabilizing a magnetic levitation system. The rest of the paper is arranged as follows. Section 2.0 considers the complete modeling of a magnetic levitation system, with both nonlinear and linearized models treated in detail. Section 3.0 focuses on the magnetic levitation system design and simulation, and also, shows graphical displays to buttress design results. And finally, Section 4.0 presents the conclusion. All the MATLAB scripts used for the design and simulation are separately given in the appendix.

2. Magnetic Levitation System Modelling

2.1 Layout of the System

The layout of a typical magnetic levitation system is illustrated in Fig. 1 (Al-Muthairi and Zribi, 2004). This arrangement involves the adjustment of magnetic energy or force in order to balance or counteract the gravitational pull exerted on an object (a small light ferromagnetic ball in this case).

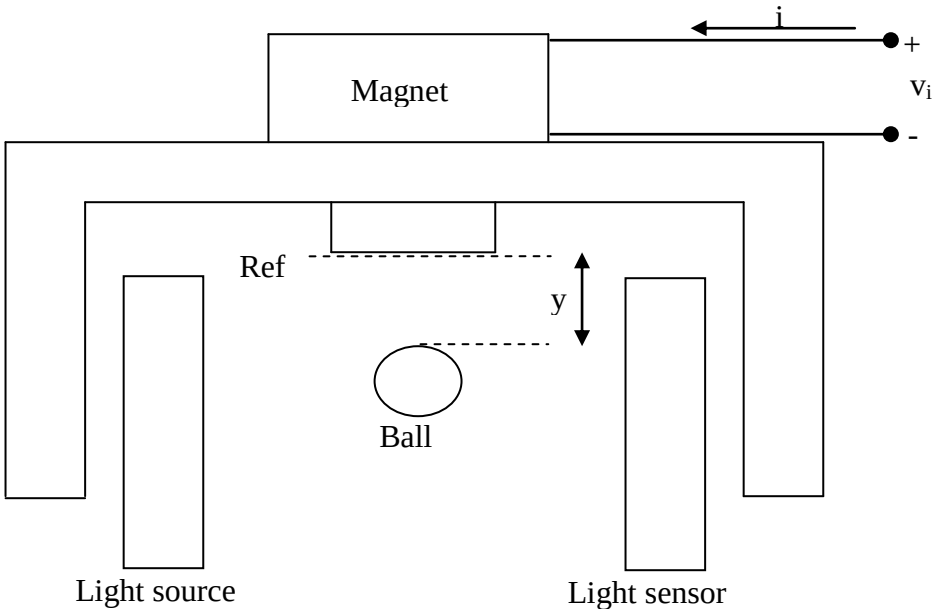

Fig. 1: Schematic of a magnetic levitation system

Restricted to the vertical direction only, the motion of the ball is monitored by a properly arranged pair of a light emitter and a light detector so that the instantaneous position of the ball can be fed back for the purpose of control computation. This control effort (generated by an electromagnetic circuit) is to ensure that the ball is brought to, and kept at, a desired position. As the ball's position deviates, due to an external disturbance, from the set point, the sensor output changes accordingly so that the right amount of control effort is computed and used to bring the ball back to the set point and keep it there.

Fig. 2 is the representation of the electric circuit subsystem of the magnetic levitation system. It is a series combination of a linear resistor, with resistance R, and a non-linear inductor, with inductance L(y).

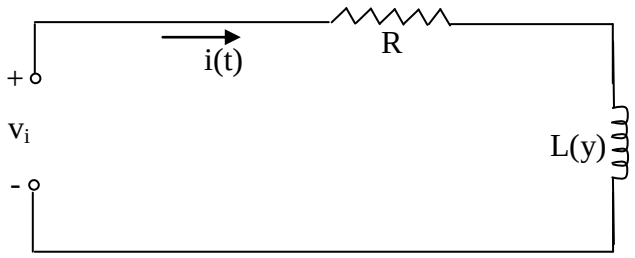

Fig. 2: An electric circuit subsystem of the maglev system.

The inductance is non-linear due to the variable reluctance of the magnetic circuit—the reluctance is directly proportional to the distance between the electromagnet and the ball, implying that as this distance decreases (i.e., ball's approaching the magnet), the inductance increases, and vice versa.

2.2 Non-linear Model of the System

To determine the complete model of this system, two important dynamic equations, one representing the variations of the magnetic flux with time (based on Fig. 2) and the other the Newtonian equation of

motion of the ball based on forces acting on it as shown in Fig. 3, are required.

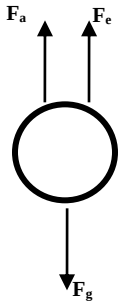

Fig. 3: A free-body diagram showing forces acting on the ball.

From Fig. 2, it can be written that

$$\frac{d\phi(t,y)}{dt} + Ri(t) = v_i \qquad 1$$

where $\phi(t, y)$ is the magnetic flux in webers, i(t) is the current in amperes, R is the resistance in ohms, v_i is the source voltage in volts, and t is time in seconds.

Since the magnetic flux around a coil is directly proportional to the current flow in the coil, with the coil inductance being a factor of proportionality, thus,

$$\phi(t,y) = L(y)i(t) \qquad 2$$

Differentiating (2) with respect to time and substituting the result into (1) yield

$$L(y)\frac{di(t)}{dt} + \frac{dL(y)}{dy}.\frac{dy}{dt} + Ri(t) = v_i$$

or

$$L(y)\frac{di(t)}{dt} + \left(R + \frac{dL(y)}{dy}\frac{dy}{dt}\right)i(t) = v_i \qquad 3$$

where y(t) is the distance between the electromagnet and the ball, and L(y) is the total inductance of the circuit in henry.

Also, from Fig. 3,

$F_a + F_e = F_g \qquad 4$

where F_a is the accelerating force due to the mass of the ball, F_e is the magnetic force, and F_g is the gravitational force.

Since

$$F_a = m\frac{d^2y}{dt^2} \text{ and } F_g = mg,$$

therefore, (4) can be rewritten as

$$m\frac{d^2y}{dt^2} = mg - F_e$$

or

$$m\frac{dv}{dt} = mg - F_e \qquad 5$$

In (5), m is the mass of the ball in kg, v(= dy/dt) is the velocity of the ball in m/s, and g is the acceleration due to gravity in m/s^2.

Equations (3) and (5), which constitute the mathematical representation of the system, can be developed further by redefining L(y) and F_e and finding appropriate expressions for them, respectively, as shown by the following derivations.

L(y) represents the sum of two inductances, L_c and L_b, i.e.,

$L(y) = L_c + L_b \qquad 6$

L_c, which is fixed, is the inductance due to the electromagnet coil; L_b is the inductance due to the ball. Because L_b is inversely proportional to the distance between the electromagnet and the ball, it implies that if L_o is the inductance that corresponds to a set-point position, y_o, then the inductance, L_b, that corresponds to an instantaneous position, y, is expressed as

$$L_b = \frac{L_o y_o}{y} \qquad 7$$

Therefore, putting (7) in (6) gives

$$L(y) = L_c + \frac{L_o y_o}{y} \qquad (8)$$

Further, the magnetic force, F_e, is defined as the rate of change of work done with distance as the ball is moved from one position to the other by the force, and is given as

$$F_e = -\frac{dW}{dy} \qquad 9$$

Where

$W = \frac{1}{2}L(y)i^2$ (i.e., the energy stored in the magnetic field)

Hence, (9) gives

$$F_e = \frac{1}{2}L_o y_o \frac{i^2}{y^2} \quad (10)$$

which, with L_o and y_o fixed, can further be reduced to

$$F_e = K\frac{i^2}{y^2} \quad (11)$$

where K(called the magnetic force constant) = $\frac{1}{2}L_o y_o$

Now, substituting (8) into (3), and (11) into (5), we have

$$L(y)\frac{di(t)}{dt} + \left(R - \frac{L_o y_o}{y^2}\frac{dy}{dt}\right)i(t) = v_i \quad (12)$$

and

$$m\frac{dv}{dt} = mg - K\frac{i^2}{y^2} \quad (13)$$

The final non-linear equations are

$$\frac{di(t)}{dt} + \frac{1}{L(y)}\left(R - \frac{2K}{y^2}v\right)i(t) = \frac{1}{L(y)}v_i \quad (14)$$

$$\frac{dv}{dt} = g - \frac{K}{m}\frac{i^2}{y^2} \quad (15)$$

Let state variables and the input be defined as:

$$x_1 = y;\ x_2 = dy/dt = v;\ x_3 = i;\ u = v_i$$

The equivalent nonlinear state-space dynamic model of the system is:

$$\frac{dx_1}{dt} = x_2$$

$$\frac{dx_2}{dt} = g - \frac{K}{m}\left(\frac{x_3}{x_1}\right)^2$$

$$\frac{dx_3}{dt} = \frac{1}{L(y)}u - \left(\frac{R}{L(y)} - \frac{2K}{L(y)}\frac{x_2}{x_1^2}\right)x_3 . \quad (16)$$

2.3 Linearized Model of the System

As can be seen in the model just developed, the maglev system is non-linear. As mentioned earlier, several non-linear controllers have been designed for this system in the literature. But the focus here is on how to improve the system performance for small-range operation. Therefore, the above non-linear model is linearized about a nominal operating point, $\boldsymbol{x}_o(t)$, which corresponds to a nominal input, u_o, using a Taylor series (Kuo and Golnaraghi, 2003).

First, the model in (16) is rewritten as

$$\frac{dx_1}{dt} = f_1(x_1, x_2, x_3, u) = x_2$$

$$\frac{dx_2}{dt} = f_2(x_1, x_2, x_3, u) = g - \frac{K}{m}\left(\frac{x_3}{x_1}\right)^2 \quad (17)$$

$$\frac{dx_3}{dt} = f_3(x_1, x_2, x_3, u) = \frac{1}{L(y)}u - \left(\frac{R}{L(y)} - \frac{2K}{L(y)}\frac{x_2}{x_1^2}\right)x_3 .$$

Then expanding (17) into a Taylor series about $\boldsymbol{x}_o(t) = [x_{o1}, x_{o2}, x_{o3}]$ and ignoring terms of order higher than first result in

$$\frac{dx_i}{dt} = f_i(x_1, x_2, x_3, u)\Big|_{x_o(t),u_o} + \frac{\partial f_i(x_1, x_2, x_3, u)}{\partial x_1}\Big|_{x_o(t),u_o} (x_1 - x_{o1})$$

$$+ \frac{\partial f_i(x_1, x_2, x_3, u)}{\partial x_2}\Big|_{x_o(t),u_o} (x_2 - x_{o2}) + \frac{\partial f_i(x_1, x_2, x_3, u)}{\partial x_3}\Big|_{x_o(t),u_o} (x_3 - x_{o3})$$

$$+ \frac{\partial f_i(x_1, x_2, x_3, u)}{\partial u}\Big|_{x_o(t),u_o} (u - u_o)$$

18

where i = 1, 2, 3.

Hence,

$$\frac{dx_1}{dt} = \frac{dx_{o1}}{dt} + 0 + 1.(x_2 - x_{o2}) + 0 + 0$$

$$\frac{dx_2}{dt} = \frac{dx_{o2}}{dt} + \frac{2K}{m}\frac{{x_{o3}}^2}{{x_{o1}}^3}.(x_1 - x_{o1}) + 0 - \frac{2K}{m}\frac{x_{o3}}{{x_{o1}}^2}.(x_3 - x_{o3})$$

$$\frac{dx_3}{dt} = \frac{dx_{o3}}{dt} - \frac{4Kx_{o2}x_{o3}}{L{x_{o1}}^3}.(x_1 - x_{o1}) + \frac{2Kx_{o3}}{L{x_{o1}}^2}.(x_2 - x_{o2}) - \left(\frac{R}{L} - \frac{2Kx_{o2}}{L{x_{o1}}^2}\right)(x_3 - x_{o3})$$

$$+ \frac{1}{L}(u - u_o)$$

19

Noting that

$$\Delta x_i = x_i - x_{oi} \;;\; \frac{d\Delta x_i}{dt} = \frac{dx_i}{dt} - \frac{dx_{oi}}{dt} \qquad (i = 1, 2, 3),$$

then, (19) becomes

$$\frac{d\Delta x_1}{dt} = \Delta x_2$$

$$\frac{d\Delta x_2}{dt} = \frac{2K}{m}\frac{{x_{o3}}^2}{{x_{o1}}^3}\Delta x_1 - \frac{2K}{m}\frac{x_{o3}}{{x_{o1}}^2}\Delta x_3$$

$$\frac{d\Delta x_3}{dt} = -\frac{4Kx_{o2}x_{o3}}{L{x_{o1}}^3}\Delta x_1 + \frac{2Kx_{o3}}{L{x_{o1}}^2}\Delta x_2 - \left(\frac{R}{L} - \frac{2Kx_{o2}}{L{x_{o1}}^2}\right)\Delta x_3 + \frac{1}{L}\Delta u$$

20

The complete linearized state-space model in matrix notation, defining the output as

$$\Delta y = \Delta x_1$$

yields

$$\begin{pmatrix} \Delta\dot{x}_1 \\ \Delta\dot{x}_2 \\ \Delta\dot{x}_3 \end{pmatrix} = \begin{pmatrix} 0 & 1 & 0 \\ \frac{2Kx_{o3}^2}{m{x_{o1}}^3} & 0 & -\frac{2Kx_{o3}}{m{x_{o1}}^2} \\ \frac{4Kx_{o2}x_{o3}}{L{x_{o1}}^3} & \frac{2Kx_{o3}}{L{x_{o1}}^2} & -\frac{R}{L} + \frac{2Kx_{o2}}{L{x_{o1}}^2} \end{pmatrix} \begin{pmatrix} \Delta x_1 \\ \Delta x_2 \\ \Delta x_3 \end{pmatrix} + \begin{pmatrix} 0 \\ 0 \\ \frac{1}{L} \end{pmatrix} \Delta u$$

$$\Delta y = \begin{pmatrix} 1 & 0 & 0 \end{pmatrix} \begin{pmatrix} \Delta x_1 \\ \Delta x_2 \\ \Delta x_3 \end{pmatrix} \qquad 21$$

Now, the nominal operating point of the system can be deduced by considering the behavior of the system at an equilibrium point.

At an equilibrium point, and referring back to (16),

$$\left.\frac{dx_i}{dt}\right|_{x_1 = x_{o1}; x_2 = x_{o2}; x_3 = x_{o3}} \equiv 0 \qquad (i = 1, 2, 3).$$

Hence,

$$\frac{dx_{o1}}{dt} = x_{o2} = 0$$

$$\frac{dx_{o2}}{dt} = g - \frac{K}{m}\left(\frac{x_{o3}}{x_{o1}}\right)^2 = 0$$

$$\frac{dx_{o3}}{dt} = \frac{1}{L(y)}u - \left(\frac{R}{L(y)} - \frac{2K}{L(y)}\frac{x_{o2}}{x_{o1}^2}\right)x_{o3} = 0, \qquad (22)$$

which implies that, given an equilibrium position, x_{o1}, of the ball,

$$x_{o2} = 0 \;\; ; \;\; x_{o3} = \left(\sqrt{\frac{mg}{K}}\right)x_{o1}$$

By substituting $x_{o2} = 0$ into (21), a simplified linearized state-space model

$$\begin{pmatrix} \dot{x}_1 \\ \dot{x}_2 \\ \dot{x}_3 \end{pmatrix} = \begin{pmatrix} 0 & 1 & 0 \\ \frac{2KI^2}{my_o^3} & 0 & -\frac{2KI}{my_o^2} \\ 0 & 0 & -\frac{R}{L_c} \end{pmatrix}\begin{pmatrix} x_1 \\ x_2 \\ x_3 \end{pmatrix} + \begin{pmatrix} 0 \\ 0 \\ \frac{1}{L_c} \end{pmatrix}u$$

$$y = \begin{pmatrix} 1 & 0 & 0 \end{pmatrix}\begin{pmatrix} x_1 \\ x_2 \\ x_3 \end{pmatrix} \qquad (23)$$

results, where $I = x_{o3}$; $y_o = x_{o1}$.

Note that the incremental symbol, Δ, has been dropped in (23). While this makes the model appear more compact, however, it does not change the meaning and interpretation of the model. Also in the same equation, L has been assumed to be equivalent to L_c since $L_c >> L_o$, and, under a properly tuned compensator, $y = y_o$.

For system design, typical parameters values used are (Shahian and Hasul, 1993):

R = 31.1Ω; L_c = 0.109H; g = 9.81m/s^2; K = 0.0006590Nm^2/A^2;

m = 0.01058kg; I = 0.125A; y_0 = 0.01m;

The transfer function of the system can be determined from (23) as

3. Magnetic Levitation System Design and Simulation

$$\frac{Y(s)}{U(s)} = \frac{-1419.6}{s^3 + 283.50s^2 - 1946.5s - 551830}$$

(The MATLAB script for finding this transfer function is shown in the appendix.)

As can be seen from (24), this system is unstable—the Routh-Hurwitz stability criterion is clearly not met. Therefore, a compensating network is required to stabilize it. The overall block diagram of the system is shown in Fig. 4. Here G(s) is the gain (or transfer function) of the plant, $G_c(s)$ is the compensator gain, $G_s(s)$ is the gain of the sensor (156V/m) (Shahian and Hasul, 1993), $V_1(s)$ is the output voltage of the desired position transducer, $V_2(s)$ is the output voltage of the sensor, E(s) is the error signal, U(s) is the compensator output, and R(s) and Y(s) are the desired and actual positions of the maglev system, respectively.

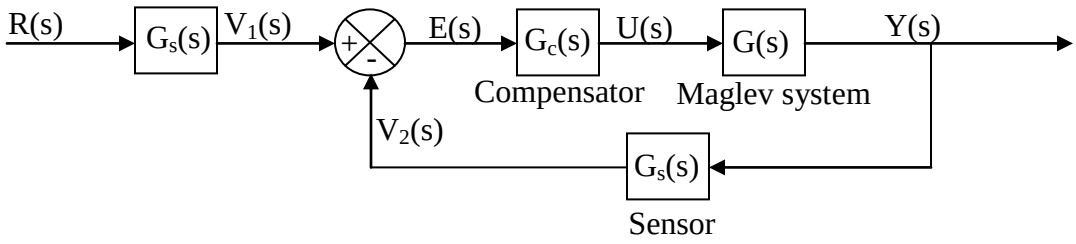

Fig. 4: Overall closed-loop representation of the maglev system

To verify whether simple gain adjustment will stabilize the system, a constant-gain compensator is used as shown in Fig. 5. The root locus for this situation is depicted in Fig. 6.

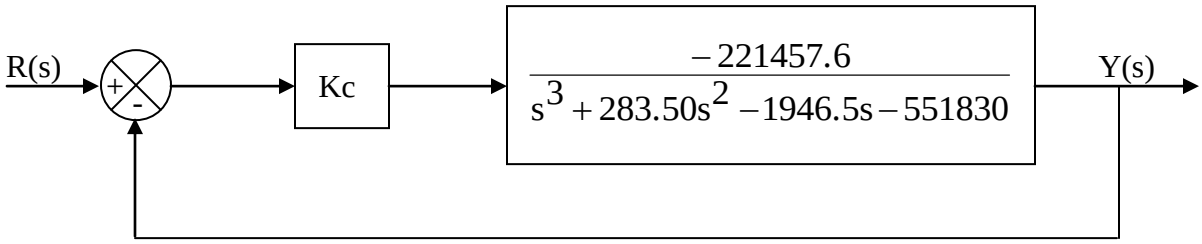

Fig. 5: Block diagram of a constant gain-compensated maglev system.

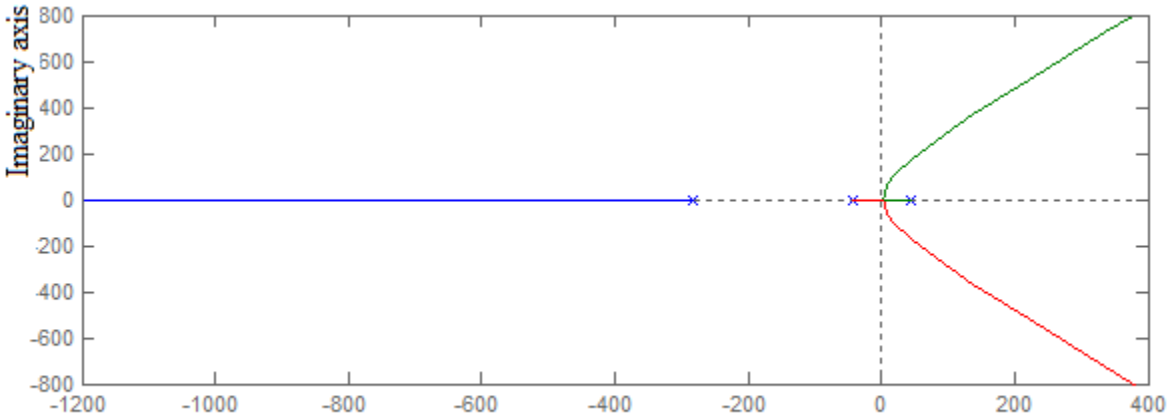

Fig. 6: The root locus of a constant gain-compensated maglev system

The root locus shows that no amount of increase in gain will result in system stability, as two of the system closed-loop poles always fall in the right-half s-plane. This is further supported by the Bode plot of the uncompensated system (shown in Fig. 7), which clearly reveals that for any value of the system gain, both the gain margin and the phase margin remain negative. (See the appendix for a MATLAB script to create these plots.) Therefore, the most important design challenge here reduces to that of stabilizing the magnetic levitation system.

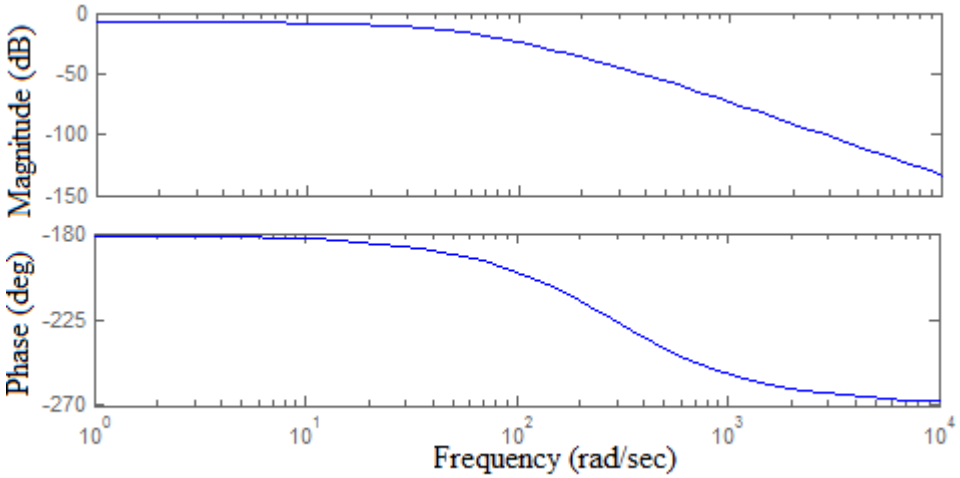

Fig. 7: The Bode plot of an uncompensated maglev system.

3.1 Root Locus Design

The maglev system can be stabilized if the uncompensated system root locus is reshaped such that a certain range of values of the system gain will make all the closed-loop poles fall in the right-half s-plane. And insightful leads from the locus show that this corrective reshaping can be effected if a zero or a combination of a zero and a pole is inserted at appropriate locations on the negative real-axis of this uncompensated root locus. This implies that a proportional-derivative (PD) or a phase-lead controller will be effective in stabilizing system. The design of these two compensators is considered here.

3.1.1 Proportional-Derivative Compensator

A general cascade proportional-derivative controller is described by the transfer function

$$G_C(s) = \frac{U(s)}{E(s)} = K_p + K_D s = K_p\left(1 + \frac{K_D}{K_p}s\right) \tag{25}$$

where K_p and K_D are the proportional and derivative constants of the controller, respectively.

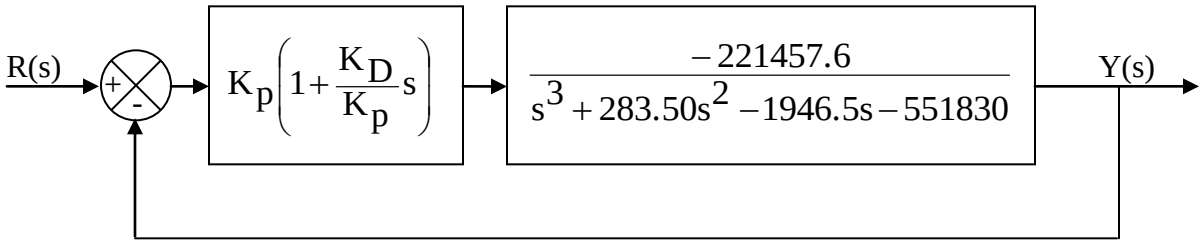

Fig. 8: Block diagram of a PD-compensated maglev system.

Combining this with the maglev system transfer function, as shown in Fig. 8, results in the open-loop transfer function

$$GH(s) = \frac{221457.6K_p\left(1+\frac{K_D}{K_p}s\right)}{s^3 + 283.50s^2 - 1946.5s - 551830} \quad 26$$

To determine the ranges of values of K_p and K_D that will ensure system stability, the popular Routh-Hurwitz criterion (Nise, 2007) is used. The analysis is shown in Table 1.

Table 1: The Routh array for PD-compensated system stability analysis

s^3	1	$221457.6K_D - 1946.5$	0
s^2	283.50	$221457.6Kp - 551830$	0
s^1	$\frac{283.50(221457.6K_D - 1946.5) - (221457.6K_p - 551830)}{283.50}$	0	0
s^0	$221457.6Kp - 551830$		

From this table, the system is stable if the condition

$$K_p > 2.4918; K_p/K_D < 283.50 \quad 27$$

is met. The information given in (27) is used to generate root loci for the system in (26) in order to obtain an appropriate combination of values of K_p and K_D that guarantees stability and gives good response. This is carried out by sweeping through various values for the ratio K_P/K_D and determining proper corresponding values for K_p. The resulting loci are displayed in Fig. 8.

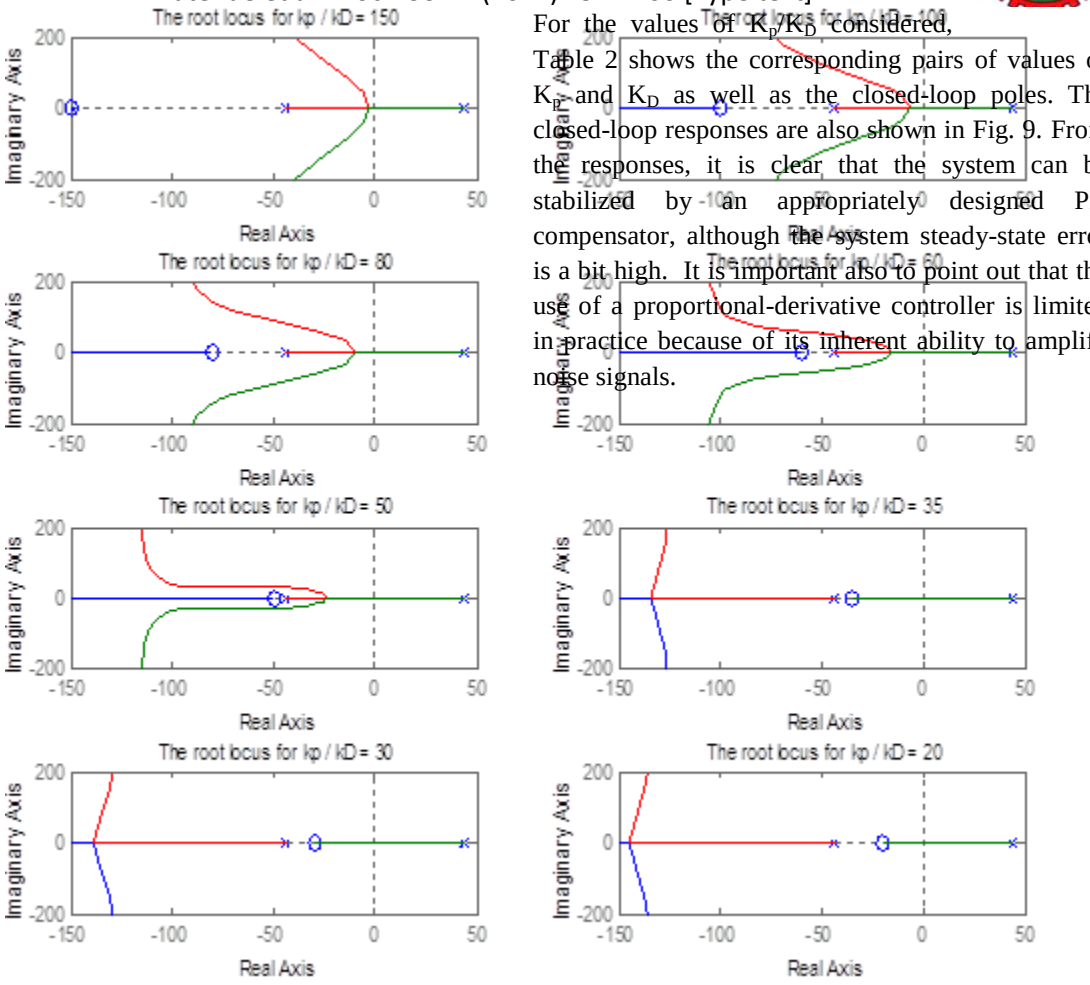

Fig. 8: Root loci for the pd-compensated maglev system for various values of Kp/KD.

For the values of K_p/K_D considered, Table 2 shows the corresponding pairs of values of K_p and K_D as well as the closed-loop poles. The closed-loop responses are also shown in Fig. 9. From the responses, it is clear that the system can be stabilized by an appropriately designed PD compensator, although the system steady-state error is a bit high. It is important also to point out that the use of a proportional-derivative controller is limited in practice because of its inherent ability to amplify noise signals.

Table 2: Selected pairs of values of K_p and K_D and corresponding closed-loop poles

K_p/K_D	K_p	K_D	Pole s_1	Poles s_1, s_2
150	22.2	0.1480	-231.74	-25.88+134.77j, -25.88-134.77j
100	16.8	0.1680	-185.51	-48.99+121.16j, -48.99-121.16j
80	14.3	0.1788	-148.64	-67.43+114.22j, -67.43-114.22j
60	8.66	0.1443	-137.38	-73.06+67.86j, -73.06-67.86j
50	5.85	0.1170	-166.28	-58.61+32.21j, -58.61-32.21j
35	10	0.2857	-31.09	-126.20+193.78j, -126.20-193.78j
30	13.1	0.4367	-26.73	-128.39+267.23j, -128.39-267.23j
20	9.14	0.4570	-15.48	-134.01+277.76j, -134.01-277.76j

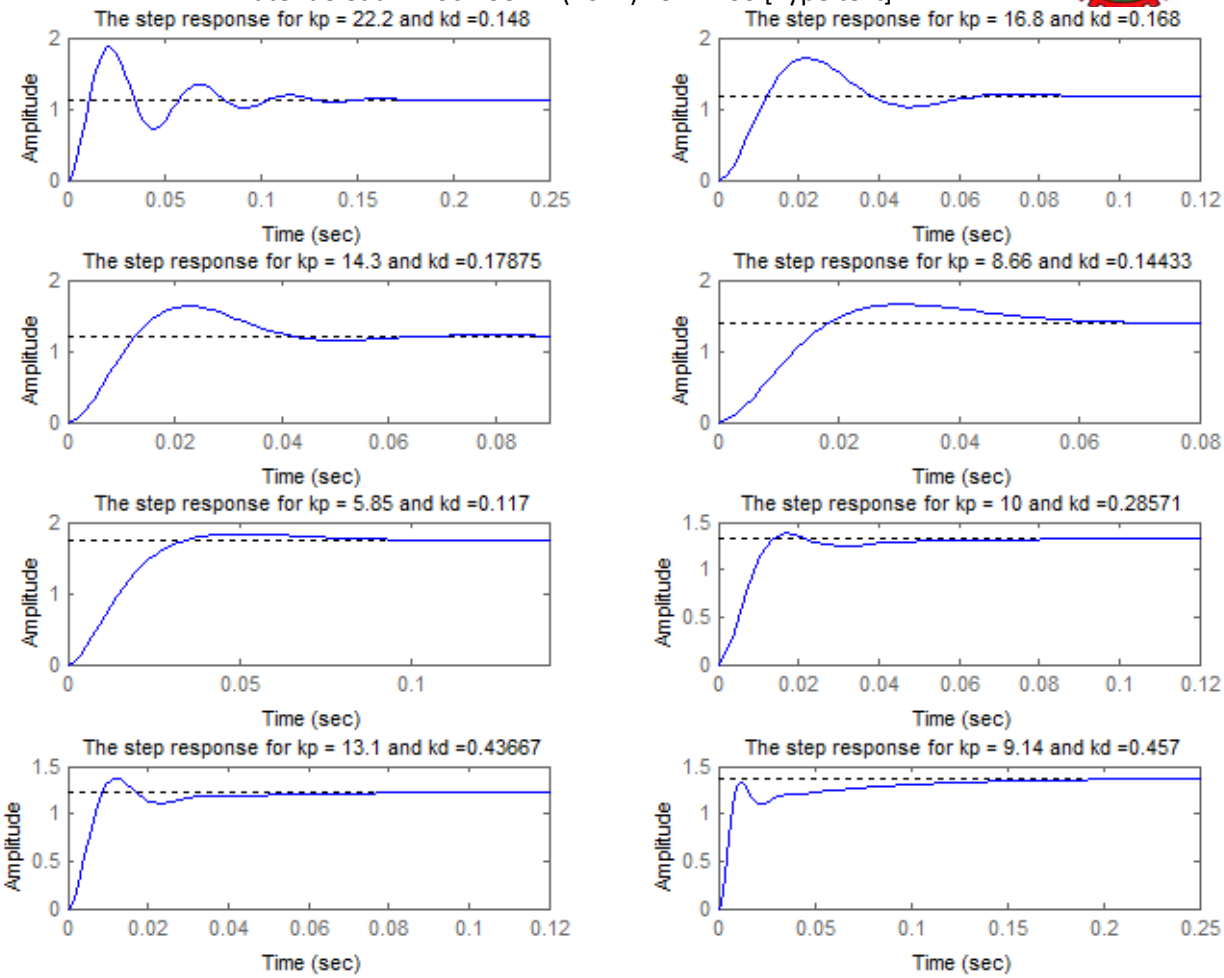

Fig. 9: Closed-loop responses for the pd-compensated maglev system.

3.1.2 Phase-Lead Compensator

As can be seen from the uncompensated maglev system root locus, a pair of a zero (located between s = 0 and s = - 44.1190) and a pole (located elsewhere in the right-half s-plane, but farther away to the left of the zero) can be used to augment the uncompensated open-loop transfer function of the maglev system in order to stabilize it. This gives rise to a phase-lead compensator. And a typical representation of a phase-lead compensator is given by

$$G_C(s) = K_C \frac{s+a}{s+b}; \quad a < b \qquad (28)$$

where K_c, a, and b are the compensator gain, zero, and pole, respectively.

If (28) is used to compensate the maglev system, the resulting open-loop transfer function becomes

$$GH(s) = \frac{221457.6K_C(s+a)}{(s+b)(s^3 + 283.50s^2 - 1946.5s - 551830)} \qquad (29)$$

The root-contour approach can be employed to find the appropriate values of K_c, a, and b, or since an

approximate range of values of 'b' is known, and the value of 'a' can be deduced based on the reasoning that the farther 'a' is from the imaginary axis (but not too close to the system open-loop pole at s = -44.1190) the better the stability, then the compensator parameters can be determined from root loci generated for varying values of K_c. The latter approach is used here.

Fig. 10 shows root loci for values of b between 44.119 and 490, and a = 35. From this figure, it is apparent that the greater the value of 'b' the farther to the left the branches of the locus between s = -44.119 and s = -283.50 (or -b) are. And for a typical pair of a = 35 and b = 290, the range of values of K_c that guarantees system stability is $24 < K_c < 212$. For these values of a and b, and a selected set of values of K_c, the closed-loop poles are given in Table 3 while the closed-loop responses are displayed in Fig. 11.

Table 3: Selected values of K_c and the corresponding closed-loop poles for a = 35; b=290

K_c	Poles s_1, s_2, s_3, s_4			
30	-408.98;	-71.17 -68.99j;	-71.17 +68.99j;	-22.17
40	-425.34;	-59.37 - 101.15j;	-59.37 +101.15j	-29.42
50	-439.38;	-50.98 -124.34j;	-50.98 +124.34j;	-32.16
60	-451.79;	-44.09 -142.77j;	-44.09 +142.77j;	-33.53
70	-463.00;	-38.08 - 158.24j;	-38.08 +158.24j;	-34.35
80	-473.25;	-32.68 - 171.69j;	-32.68 +171.69j;	-34.89
90	-482.74;	-27.74 - 183.65j;	-27.74 +183.65j;	-35.27
100	-491.59;	-23.17 -194.47j;	-23.17 +194.47j;	-35.56
120	-507.77;	-14.89 - 213.54j;	-14.89 +213.54j;	-35.95
130	-515.23;	-11.09 - 222.09j;	-11.09 +222.09j;	-36.10

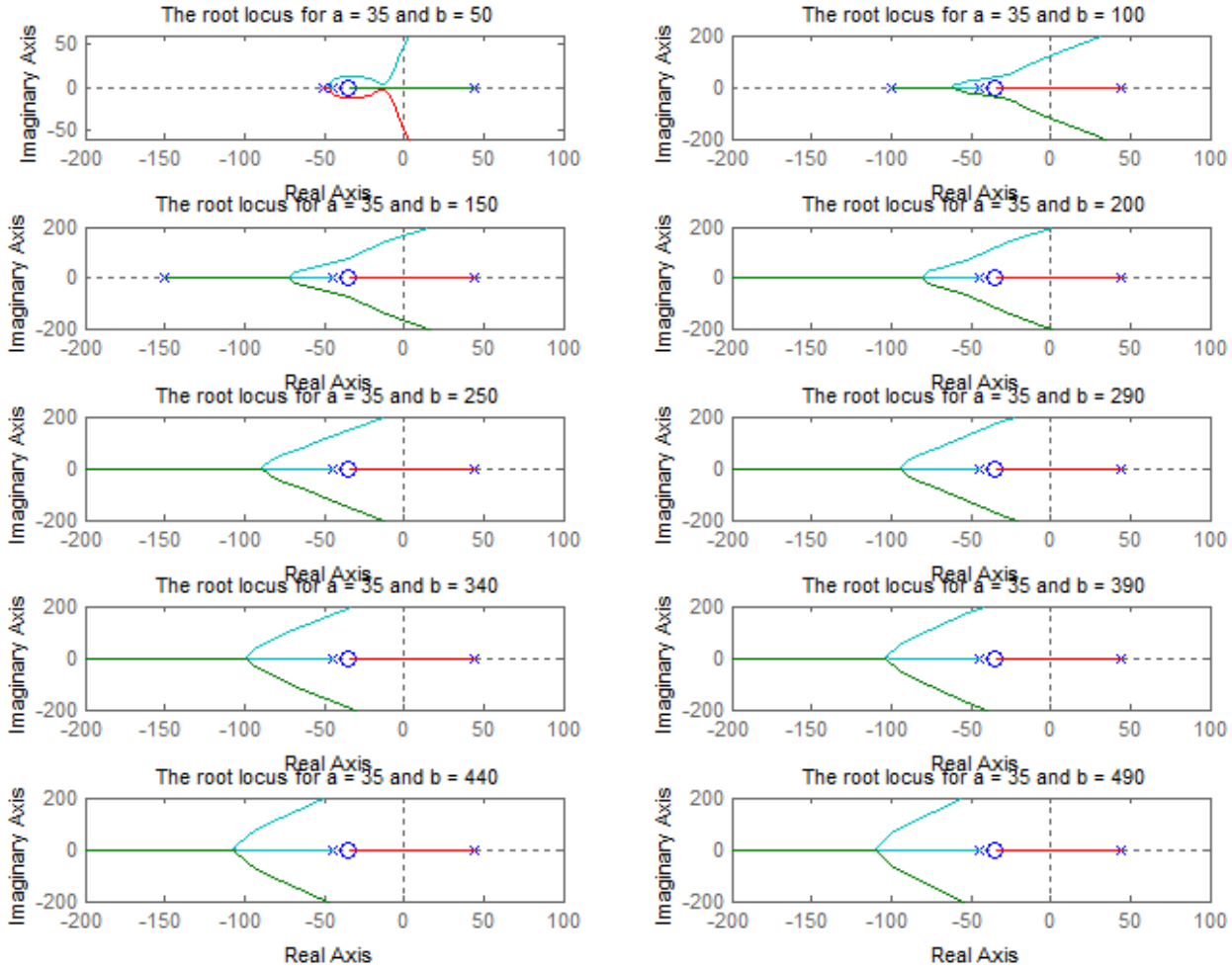

Fig. 10: Root loci for a = 35, and various values of b.

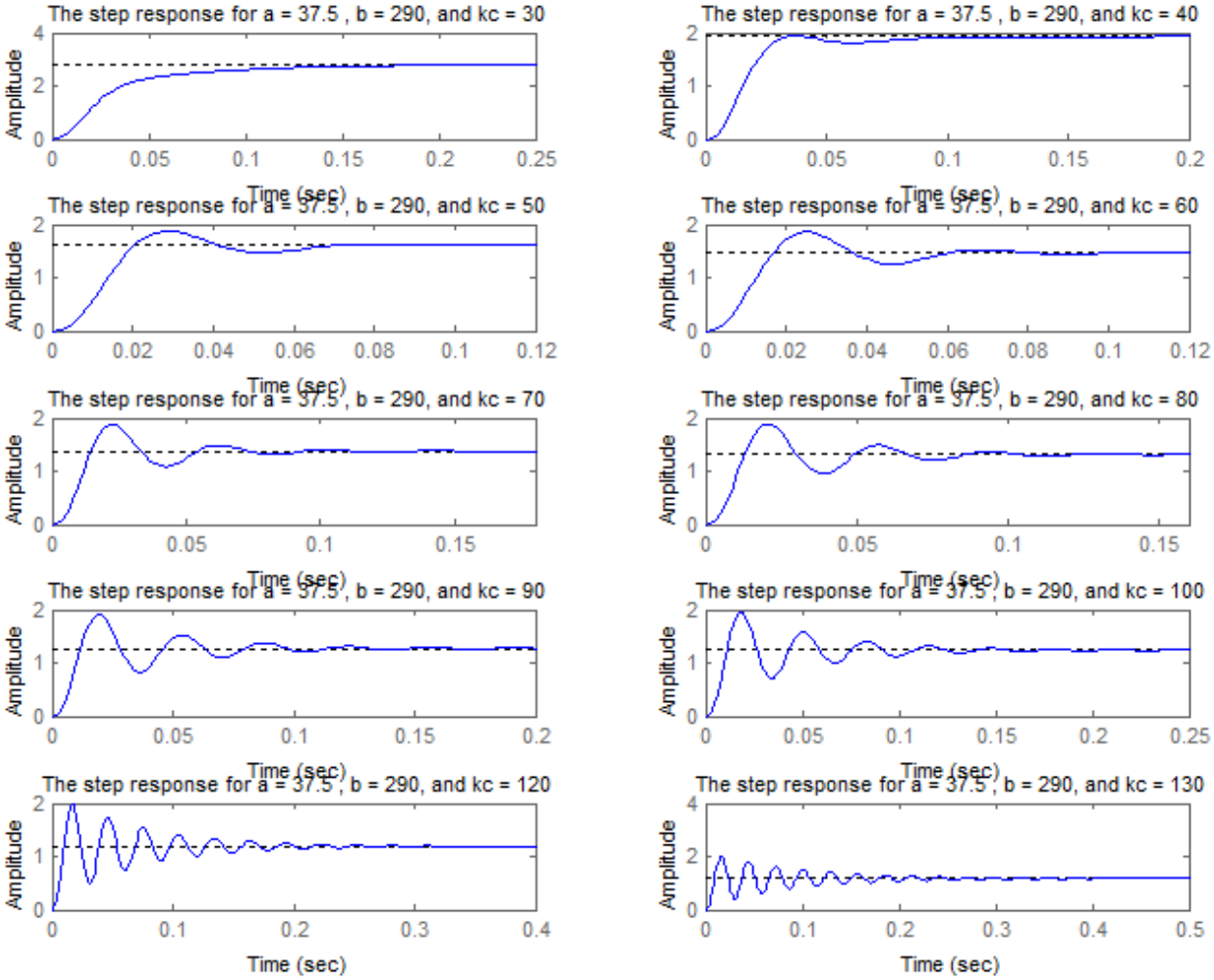

Fig. 11: Closed-loop step responses for a phase lead compensated maglev system.

4. Conclusion

Stabilization of a magnetic levitation system has been the focus of this paper. Although the system is an unstable nonlinear one, it is clear that a linear compensator can be designed to stabilize it if its operation is limited to a small range. We develop a complete nonlinear model of the system, and then form an approximate linearized equivalent from it. Based on this linearized model, we consider two linear compensators—proportional-derivative and phase lead—and show that the magnetic levitation system can be stabilized by an appropriate selection of the parameters of the compensators using a classical design approach aided by a computer software tool. We compute and present the closed-loop poles of each design and the corresponding step responses, and also show the system stability limits. This approach proves quite useful and effective, as several simulation runs can be performed quickly to expedite the design. However, for a large-range operation, a more robust controller will be required to effectively bring the system into a region of stability. And for this latter type of controllers, several strategies have been employed and are available in the literature, while the maglev system continues to attract more research attention.

Appendix

The various MATLAB scripts used in this tutorial are highlighted below.

A. Computation of the maglev system transfer function

```
% This script computes the
transfer function of a maglev
system using
% Y/U=C((SI-A)^-1)B.
syms s
% Define the parameters of the
model.
R = 31.1; Lc = 0.1097; g = 9.81; K
= 0.00065906;m = 0.01058;I =
0.125;
y0 = 0.01;
% Compute the values of A, B, and
C.
A=[0 1 0;(2*K*I^2)/(m*y0^3) 0 -
(2*K*I)/(m*y0^2);0 0 -R/Lc];B=[0 0
1/Lc]';
C=[1 0 0];
% Find the transfer function, Y/U.
id=eye(3,3);
disp('The transfer function is:')
Tfunction=C*(inv(s*id-A))*B
% Find the simplified transfer
function, Y/U.
[numTfunc,denTfunc]=numden(Tfuncti
on);numTfunc=sym2poly(numTfunc);
denTfunc=sym2poly(denTfunc);numTfu
nction=numTfunc/denTfunc(1);
denTfunction=denTfunc/denTfunc(1);
disp('While the simplified
transfer function is now')
tf(numTfunction,denTfunction)
```

B. The Root locus and bode plots of the uncompensated maglev system

```
% This script plots the root locus
and the bode diagram of the maglev
% system when compensated by a
constant gain.
fnum=1419.6*156;fden=[1 283.50 -
1946.55 -551830];
sys1=tf(fnum,fden);
figure(1)
rlocus(sys1)
figure(2)
bode(sys1)
```

C. The root loci for simulating the pd-compensated maglev system

```
% Script for simulating the root
locus-based pd-compensated design
kp_kd=[150 100 80 60 50 35 30 20];
L=length(kp_kd);
sysden=[1 283.50 -1946.5 -551830];
i=1;
while(i<=L)
    f=kp_kd(i);
    sysnum=221457.6*[0 0 1/f 1];
    subplot(4,2,i)
    rlocus(sysnum, sysden)
    str=['The root locus for kp /
kD = ' num2str(f)];
    title(str)
    axis([-150 50 -200 200]);
    i=i+1;
end
```

D. Closed-loop poles and step responses of the pd-compensated maglev system

```
% Script for generating the
closed-loop poles as well as the
responses of
% the pd-compensated maglev
system.
kp_kd=[150 100 80 60 50 35 30 20];
kp=[22.2 16.8 14.3 8.66 5.85 10
13.1 9.14];
kd=kp./kp_kd;
L=length(kp_kd);
sysden=[1 283.50 -1946.5 -551830];
sys2=1;syspoles=zeros(8,3);
i=1;
while(i<=L)
    f1=kp_kd(i);f2=kp(i);
    sysnum=f2*221457.6*[0 0 1/f1
1];
    sys1=tf(sysnum,sysden);
    sysfun=feedback(sys1,sys2);
    syspole=eig(ss(sysfun))';
    syspoles(i,1:3)=syspole;
    subplot(4,2,i)
    step(sysfun)
    str=['The step response for kp
= ' num2str(f2) ' and kd ='...
    num2str(f1)];
    title(str)
    i=i+1;
end
disp('The closed-loop poles are:')
syspoles;
```

E. The root loci for simulating the phase lead-compensated maglev system

```
% Script for simulating the root
locus-based phase lead-compensated
design.
a=35;
sysnum=221457.6*[0 0 0 1 a];
sysden1=[1 283.50 -1946.5 -
551830];
b=[50 100 150 200 250 290 340 390
440 490];
Lb=length(b);
i=1;clf;
while(i<=Lb)
```

```
    f1=b(i);
    sysden=conv([1 f1],sysden1);
    figure(3)
    subplot(5,2,i)
    rlocus(sysnum, sysden)
    str=['The root locus for a = '
num2str(a) ' and b = '
num2str(f1)];
    title(str)
    axis([-200 100 -200 200])
    i=i+1;
end
```

F. Closed-loop poles and step responses of the phase lead-compensated maglev system

```
% Script for generating the
closed-loop poles as well as the
responses of
% the pase lead-compensated maglev
system when b = 290.
a=37.5;
b=290;
kc=[30 40 50 60 70 80 90 100 120
130];
L=length(kc);
sys2=1;syspoles=zeros(10,4);
i=1;
while(i<=L)
    f1=kc(i);
    sysnum=f1*221457.6*[0 0 0 1
a];
    sysden=conv([1 b],[1 283.50 -
1946.5 -551830]);
    sys1=tf(sysnum,sysden);
    sysfun=feedback(sys1,sys2);
    syspole=eig(ss(sysfun))';
    syspoles(i,1:4)=syspole;
    figure(5)
    subplot(5,2,i)
    step(sysfun)
    str=['The step response for a
= ' num2str(a)' , b = '
num2str(b)',...
    and kc = ' num2str(f1)];
    title(str)
    i=i+1;
end
disp('The closed-loop poles are:')
syspoles
```

References

Al-Muthairi N. F., and Zribi M., "Sliding mode control of a magnetic levitation system," Mathematical Problems in Engineering 2004, vol. 2, 2004, pp. 93-107.

Feedback Instrument Limited, Magnetic levitation system—getting started, http://www.fdb.com, 18th September, 2012.

Franklin G.F., Powell J.D., and Workman M., Digital Control of Dynamic Systems, Addison Wesley Longman, Inc., 1998, pg. 273.

Green S.A., Hirsch R.S., and Craig K.C., "Magnetic levitation device as teaching aid for mechatronics at Rensselaer," Proc. ASME Dynamic Systems and Control Division, vol. 57-2, 1995, pp. 1047–1052.

Kuo B. C., and Golnaraghi F., Automatic Control Systems, John Wiley & Sons (Asia) Pte. Ltd., 2003, pp. 110-111.

Naumivic M. B., Veselic B. R., "Magnetic levitation system in control engineering education," Automatic Control and Robotics, vol. 7, no.1, 2008, pp. 151-160.

Nise N. S., Control Systems Engineering, Wiley India (P.) Ltd., Delhi, Third Reprint, 2007, pp. 329-352.

Shahian B., and Hassul M., Control System Design Using MATLAB. Englewood Cliffs: Prentice Hall, 1993, pp. 455–465.